Available online at www.sciencedirect.com
ScienceDirect
Journal of Sound and Vibration 305 (2007) 85–96
JOURNAL OF SOUND AND VIBRATION
www.elsevier.com/locate/jsvi

Exact convergence studies on static and dynamic analyses of plates by using the double U-transformation and the finite-element method

Y. Yang[a], J.K. Liu[b,*], P.Y. Huang[a]

[a]College of Traffic and Communications, South China University of Technology, Guangzhou 510641, PR China
[b]Department of Mechanics, Zhongshan University, Guangzhou 510275, PR China

Received 22 November 2005; received in revised form 25 May 2006; accepted 17 March 2007

Abstract

This paper presents exact static and dynamic analyses of simply supported rectangular plates. The analytical solutions for displacements, natural frequencies and dynamic responses are obtained by using the double U-transformation and the finite-element method. These explicit solutions then can easily be used to accurately study the convergence rates of the finite-element solutions. Two non-conforming plate elements are taken as examples to demonstrate the proposed procedure. The analytical finite-element solutions, the exact error expressions and convergence rates are derived. Moreover, the convergent speeds of the two elements are discussed.

1. Introduction

The finite-element method is an important numerical calculation method in engineering structural analysis. How to improve the efficiency and precision of the finite-element formula is a big problem and always attracts the attention of computing mathematicians and dynamicists. Dividing elements to less size and increasing the degree of the interpolation polynomial can only decrease the error but not improve the precision. So it is important to uncover the convergence of the finite element. Scientists have found some methods to verify the convergence of the finite element, such as patch test and convergence criterions. The studies can estimate the error in grade, for example, the error of some finite element is $O(n)$ or $O(n^2)$, or others, but cannot give out the error in exactness. This paper uses the U-transformation method to discuss the convergence of some finite-element formula and give out the explicit convergence rates and the coefficients of the main error.

The U-transformation method is an analytical method for the exact analysis of structures with periodic property. By performing U-transformation on a cyclic periodic structure, the governing equations with continuity conditions can be uncoupled to a set of independent equations. In the last 20 years, the method has been applied to study the static and dynamic problems of structures with periodicity [1], periodicity in two

*Corresponding author.
E-mail address: jikeliu@hotmail.com (J.K. Liu).

0022-460X/$ - see front matter © 2007 Elsevier Ltd. All rights reserved.
doi:10.1016/j.jsv.2007.03.035

dimensions [3], bi-periodicity [2] and nearly periodicity [4]. Recently, Liu et al. [5] extended this method to the convergence studies of the finite-difference method. The static analysis of a simply supported beam subjected to uniformly distributed loads was performed and exact convergence rates of difference solutions were obtained by using the one-dimensional finite-difference formula. More recently, Liu et al. [6] investigated the convergence rates of the two-dimensional difference formula. In 1993, Chan et al. [7] applied the U-transformation method to analyze the simply supported plates by using the Timoshenko plate element, and the explicit finite-element solutions for dynamic problems were derived.

The present paper extends the method to the convergence study of the finite elements. The convergence rates of the displacements, natural frequencies and dynamic response functions of a simply supported plate are studied by using two non-conforming rectangular elements. By adopting the double U-transformation technique, the finite-element equations can be uncoupled to a set of independent equations, and then the analytical expressions of finite-element solutions are easily obtained. The convergence of the two finite elements can be discussed simply and effectively from the explicit solutions obtained by the proposed procedure.

2. Analytical solutions for the finite-element equation

2.1. Uncoupling of the governing equation

A rectangular plate with all edges simply supported is considered. The structure may be divided into $n \times m$ equal rectangular elements, as shown in Fig. 1. L_1, L_2 denote the lengths of the plate and a, b denote the lengths of an element in the x- and y-directions, respectively, as shown in Fig. 2. $F_{(j,k)}$ is the loading function acting on the element (j, k), and j, k are the element numbers, and it may be any distributed load. Now the plate may be regarded as a periodic structure in two directions.

In order to analyze the explicit results of static and dynamic problems by using the U-transformation method, the original system must be extended to a cyclic periodic system. Let us consider the extended structure (see Fig. 3) whose length and width are twice that of the actual ones. Moreover, the anti-symmetrical loads about the right side and lower side of actual plate must be applied on the corresponding extended part. The right and left sides and the upper and lower sides can be imagined to be connected. Then we regard the extended plate as one having cyclic periodicity in the x- and y-directions [7]. The boundary conditions of the original plate will be satisfied automatically so that an equivalent system is produced and the supports may be removed. Now we can study the equivalent system instead of the actual system.

The static equation of the element (j, k) can be expressed as [8]

$$\mathbf{K}^e \boldsymbol{\delta}^e_{(j,k)} = \mathbf{F}_{(j,k)}, \quad j = 1, 2, \ldots, 2n, \quad k = 1, 2, \ldots, 2m, \tag{1}$$

where $\mathbf{K}^e$ is the stiffness matrix and may be expressed as a symmetric cyclic matrix, $\boldsymbol{\delta}^e_{(j,k)}$ and $\mathbf{F}_{(j,k)}$ denote the displacement and loading for the element (j, k), i.e.,

$$\boldsymbol{\delta}^e_{(j,k)} = \left\{ \boldsymbol{\delta}_1^{\mathrm{T}} \quad \boldsymbol{\delta}_2^{\mathrm{T}} \quad \boldsymbol{\delta}_3^{\mathrm{T}} \quad \boldsymbol{\delta}_4^{\mathrm{T}} \right\}^{\mathrm{T}}_{(j,k)} \tag{2}$$

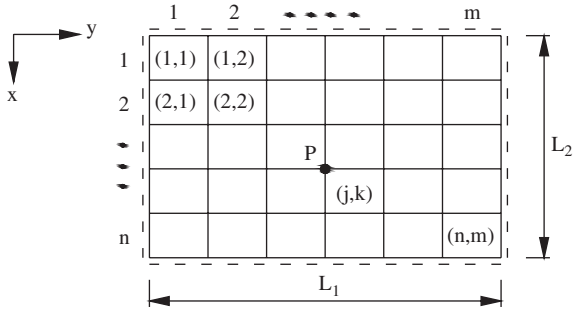

Fig. 1. Rectangular plate with simply supported edges.

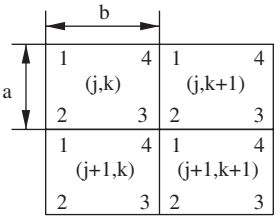

Fig. 2. Node numbers of element.

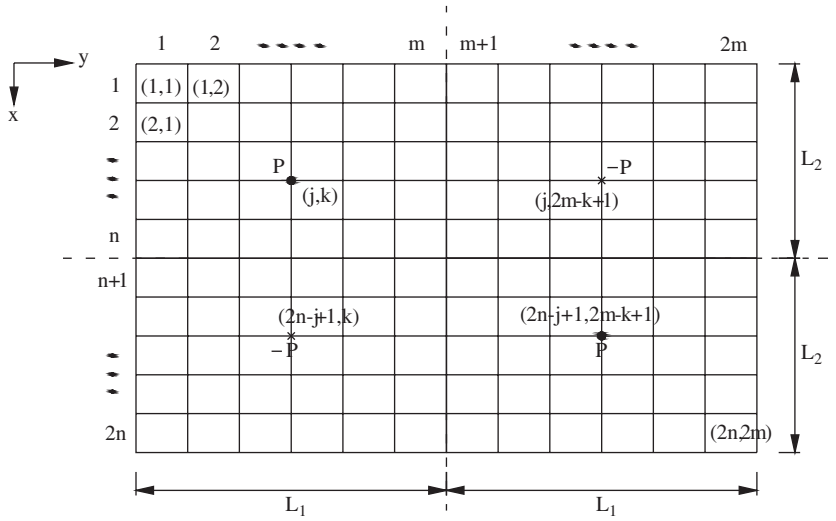

Fig. 3. Equivalent system with $2n \times 2m$ elements.

with the vector components

$$\boldsymbol{\delta}_i = \left\{ w_i \quad \theta_{xi} \quad \theta_{yi} \right\}^{\mathrm{T}}, \quad i = 1,2,3,4 \tag{3}$$

in which w_i, θ_{xi} and θ_{yi} denote the deflection and two angular rotations about x- and y-axes of node i (see Fig. 4).

From the cyclic periodicity in two directions, the following conditions need to be satisfied:

$$\begin{aligned} &\boldsymbol{\delta}_{2(j,k)} = \boldsymbol{\delta}_{1(j+1,k)}, \quad \boldsymbol{\delta}_{3(j,k)} = \boldsymbol{\delta}_{1(j+1,k+1)}, \quad \boldsymbol{\delta}_{4(j,k)} = \boldsymbol{\delta}_{1(j,k+1)}, \\ &\boldsymbol{\delta}_{1(2n+1,k)} = \boldsymbol{\delta}_{1(1,k)}, \quad \boldsymbol{\delta}_{1(2n+1,2m+1)} = \boldsymbol{\delta}_{1(1,1)}, \quad \boldsymbol{\delta}_{1(j,2m+1)} = \boldsymbol{\delta}_{1(j,1)}. \end{aligned} \tag{4}$$

Because of the cyclic periodicity, the phase difference between two adjacent substructures must be an integer times the period of the cyclic periodic structures. In order to uncouple the governing Eq. (1), the double U-transformation can be used [9,10], i.e., let

$$\boldsymbol{\delta}^e_{(j,k)} = \frac{1}{\sqrt{2n}\sqrt{2m}} \sum_{r=1}^{2n} \sum_{s=1}^{2m} \mathrm{e}^{\mathrm{i}(j-1)r\varphi_1} \, \mathrm{e}^{\mathrm{i}(k-1)s\varphi_2} \mathbf{q}_{(r,s)}, \quad j = 1,2,\ldots,2n, \quad k = 1,2,\ldots,2m \tag{5}$$

in which $\mathrm{i} = \sqrt{-1}$, and $\psi_1 = 2\pi/2n$, $\psi_2 = 2\pi/2m$. $\mathbf{q}_{(r,s)}$ is the generalized displacement matrix with the vector components:

$$\mathbf{q}_{(r,s)} = \left\{ \mathbf{q}_1^{\mathrm{T}} \quad \mathbf{q}_2^{\mathrm{T}} \quad \mathbf{q}_3^{\mathrm{T}} \quad \mathbf{q}_4^{\mathrm{T}} \right\}^{\mathrm{T}}_{(r,s)}, \quad r = 1,2,\ldots,2n, \quad s = 1,2,\ldots,2m, \tag{6}$$

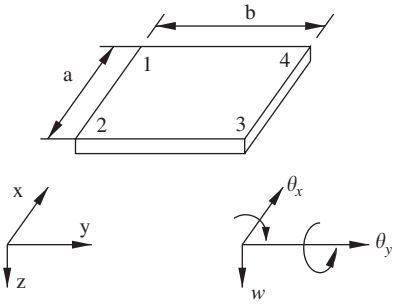

Fig. 4. Rectangular plate element with four nodes and 12 DOF.

$$\mathbf{q}_j = \left\{ q_j^1 \quad q_j^2 \quad q_j^3 \right\}^{\mathrm{T}}, \quad j = 1,2,3,4. \tag{7}$$

Applying the double U-transformation (5) into Eq. (4), the continuous conditions become

$$\mathbf{q}_{2(r,s)} = \mathrm{e}^{\mathrm{i}r\psi_1}\mathbf{q}_{1(r,s)}, \quad \mathbf{q}_{3(r,s)} = \mathrm{e}^{\mathrm{i}(r\psi_1+s\psi_2)}\mathbf{q}_{1(r,s)}, \quad \mathbf{q}_{4(r,s)} = \mathrm{e}^{\mathrm{i}s\psi_2}\mathbf{q}_{1(r,s)}. \tag{8}$$

So Eq. (6) may be rewritten as

$$\mathbf{q}_{(r,s)} = \mathbf{T}_{(r,s)}\mathbf{q}_{1(r,s)}, \tag{9}$$

where

$$\mathbf{T}_{(r,s)} = \left[\mathbf{I}_3 \quad \mathrm{e}^{\mathrm{i}r\psi_1}\mathbf{I}_3 \quad \mathrm{e}^{\mathrm{i}(r\psi_1+s\psi_2)}\mathbf{I}_3 \quad \mathrm{e}^{\mathrm{i}s\psi_2}\mathbf{I}_3 \right]^{\mathrm{T}} \tag{10}$$

and $\mathbf{I}_3$ is a unit matrix of order three.

Applying the double U-transformation (5) to the governing Eq. (1) results in

$$\mathbf{K}^*_{(r,s)}\mathbf{q}_{1(r,s)} = \mathbf{f}^*_{(r,s)}, \quad r = 1,2,\ldots,2n, \quad s = 1,2,\ldots,2m \tag{11}$$

in which

$$\mathbf{K}^*_{(r,s)} = \bar{\mathbf{T}}^{\mathrm{T}}_{(r,s)}\mathbf{K}^e\mathbf{T}_{(r,s)} = \begin{bmatrix} k^*_{11} & k^*_{12} & k^*_{13} \\ k^*_{21} & k^*_{22} & k^*_{23} \\ k^*_{31} & k^*_{32} & k^*_{33} \end{bmatrix}, \tag{12}$$

$$\mathbf{f}^*_{(r,s)} = \bar{\mathbf{T}}^{\mathrm{T}}_{(r,s)}\mathbf{f}_{(r,s)} = \left\{ f^*_1 \quad f^*_2 \quad f^*_3 \right\}^{\mathrm{T}}_{(r,s)}, \tag{13a}$$

$$\mathbf{f}_{(r,s)} = \frac{1}{\sqrt{2n}\sqrt{2m}} \sum_{j=1}^{2n}\sum_{k=1}^{2m} \mathrm{e}^{\mathrm{i}(j-1)r\varphi_1}\,\mathrm{e}^{\mathrm{i}(k-1)s\varphi_2}\mathbf{F}_{(j,k)}, \tag{13b}$$

$\mathbf{f}^*_{(r,s)}$ is the generalized loading vector.

Eq. (11) is made up of $2n \times 2m$ independent sets of equations with three variables, so the governing Eq. (1) is uncoupled. Corresponding to Eqs. (11)–(13), $\mathbf{q}_{1(r,s)}$ can be obtained as

$$q^1_{1(r,s)} = \frac{f^*_1k^*_{22}k^*_{33} + f^*_2k^*_{13}k^*_{32} + f^*_3k^*_{12}k^*_{23} - f^*_1k^*_{23}k^*_{32} - f^*_2k^*_{12}k^*_{33} - f^*_3k^*_{13}k^*_{22}}{k^*_{11}k^*_{22}k^*_{33} + k^*_{12}k^*_{23}k^*_{31} + k^*_{13}k^*_{21}k^*_{32} - k^*_{11}k^*_{23}k^*_{32} - k^*_{12}k^*_{21}k^*_{33} - k^*_{13}k^*_{22}k^*_{31}}, \tag{14a}$$

$$q^2_{1(r/s)} = \frac{f^*_1k^*_{31}k^*_{23} + f^*_2k^*_{12}k^*_{33} + f^*_3k^*_{13}k^*_{21} - f^*_1k^*_{21}k^*_{33} - f^*_2k^*_{13}k^*_{31} - f^*_3k^*_{11}k^*_{23}}{k^*_{11}k^*_{22}k^*_{33} + k^*_{12}k^*_{23}k^*_{31} + k^*_{13}k^*_{21}k^*_{32} - k^*_{11}k^*_{23}k^*_{32} - k^*_{12}k^*_{21}k^*_{33} - k^*_{13}k^*_{22}k^*_{31}}, \tag{14b}$$

$$q^3_{1(r,s)} = \frac{f^*_1k^*_{21}k^*_{32} + f^*_2k^*_{12}k^*_{31} + f^*_3k^*_{11}k^*_{22} - f^*_1k^*_{31}k^*_{22} - f^*_2k^*_{11}k^*_{32} - f^*_3k^*_{12}k^*_{21}}{k^*_{11}k^*_{22}k^*_{33} + k^*_{12}k^*_{23}k^*_{31} + k^*_{13}k^*_{21}k^*_{32} - k^*_{11}k^*_{23}k^*_{32} - k^*_{12}k^*_{21}k^*_{33} - k^*_{13}k^*_{22}k^*_{31}}. \tag{14c}$$

Now every nodal displacement of elements can be obtained from the double U-transformation (5) with Eqs. (2), (3), (6), (7) and (14), i.e.,

$$\begin{Bmatrix} w_1 \\ \theta_{x1} \\ \theta_{y1} \end{Bmatrix}_{(j,k)} = \frac{1}{\sqrt{2n}\sqrt{2m}} \sum_{r=1}^{2n} \sum_{s=1}^{2m} e^{i(j-1)r\varphi_1} e^{i(k-1)s\varphi_2} \begin{Bmatrix} q^1_{1(r,s)} \\ q^2_{1(r,s)} \\ q^3_{1(r,s)} \end{Bmatrix}, \quad j = 1,2,\ldots,2n, \quad k = 1,2,\ldots,2m. \tag{15}$$

2.2. Central deflection

In the case of a concentrated load of magnitude P acting at the center of the plate, if n and m are even, the element loading vectors for the equivalent system may be expressed as

$$\mathbf{F}_{(n/2+1,m/2+1)} = \mathbf{F}_{(n+n/2+1,m+m/2+1)} = -\mathbf{F}_{(n+n/2+1,m/2+1)} = -\mathbf{F}_{(n/2+1,m+m/2+1)} = \{ P \quad 0 \quad 0 \quad \cdots \quad 0 \}^{\mathrm{T}}_{12\times 1} \tag{16}$$

with other element loading vectors being zero. Substituting Eq. (16) into Eq. (13) yields

$$\mathbf{f}^*_{(r,s)} = \frac{-2P}{\sqrt{nm}} \sin\frac{r\pi}{2} \sin\frac{s\pi}{2} \{ 1 \quad 0 \quad 0 \}^{\mathrm{T}}, \quad r = 1,2,\ldots,2n, \quad s = 1,2,\ldots,2m. \tag{17}$$

For the same way, the generalized load matrix when the structure subjected to uniformly distributed load p_0 may be obtained as

$$\mathbf{f}^*_{(r,s)} = \frac{2p_0ab}{\sqrt{nm}} \begin{Bmatrix} -ctg\dfrac{r\varphi_1}{2} ctg\dfrac{s\varphi_2}{2} \\ -\dfrac{b}{6} i\, ctg\dfrac{r\varphi_1}{2} \\ -\dfrac{a}{6} i\, ctg\dfrac{s\varphi_2}{2} \end{Bmatrix}, \quad r \text{ and } s \text{ are odd},$$

$$\mathbf{f}^*_{(r,s)} = 0, \quad r \text{ or } s \text{ is even}. \tag{18}$$

Consider the simple case of a square plate with $n \times n$ uniform elements. Now we have $L_1 = L_2 = L$, $a = b = L/n$, and $\varphi_1 = \varphi_2 = \pi/n$. According to Eq. (15), when the structure subjected to the two loads described upper, the max deflection occuring at the center of the plate may be expressed as

$$w_{\mathrm{mid}} = \frac{1}{2n} \sum_{r=1}^{2n} \sum_{s=1}^{2n} e^{i(r\pi/2)} e^{i(s\pi/2)} q^1_{1(r,s)}. \tag{19}$$

Given certain loading function, the analytical element solution of the central deflection can be obtained by Eq. (19).

2.3. Natural frequencies

When one considers the dynamic problems, the inertia force $-\mathbf{M}^e\ddot{\boldsymbol{\delta}}_{(j,k)}$ must be added into the element loading vector $\mathbf{F}_{(j,k)}$, in which $\mathbf{M}^e$ is the element mass matrix. And the dynamic equation is

$$\mathbf{K}^e\boldsymbol{\delta}^e_{(j,k)} + \mathbf{M}^e\ddot{\boldsymbol{\delta}}^e_{(j,k)} = \mathbf{F}_{(j,k)}, \quad j,k = 1,2,\ldots,2n. \tag{20}$$

In a manner similar to Section 2.1, the dynamic equation can be uncoupled as

$$\mathbf{K}^*_{(r,s)}\mathbf{q}_{1(r,s)} + \mathbf{M}^*_{(r,s)}\ddot{\mathbf{q}}_{1(r,s)} = \mathbf{f}^*_{(r,s)} \tag{21}$$

in which

$$\mathbf{M}^*_{(r,s)} = \bar{\mathbf{T}}^{\mathrm{T}}_{(r,s)}\mathbf{M}^{\mathrm{e}}\mathbf{T}_{(r,s)}. \tag{22}$$

The frequency equation may be obtained easily from Eq. (21) as

$$\left|\mathbf{K}^*_{(r,s)} - \tilde{\omega}^2_{(r,s)}\mathbf{M}^*_{(r,s)}\right| = 0, \tag{23}$$

where $\tilde{\omega}_{(r,s)}$ are natural frequencies.

Now consider the clumped mass formulation with the rotary inertia neglected: i.e.,

$$m_{1,1} = m_{4,4} = m_{7,7} = m_{10,10} = \frac{\rho a^2}{4}, \tag{24}$$

where ρ is the mass per unit area, and other elements of the mass matrix equal to zero. For this case, the complex mass matrix may be expressed as

$$\mathbf{M}^*_{(r,s)} = \rho a^2 \begin{bmatrix} 1 & 0 & 0 \\ 0 & 0 & 0 \\ 0 & 0 & 0 \end{bmatrix}. \tag{25}$$

Substituting Eq. (25) into Eq. (23), then expanding the determinant results in

$$\tilde{\omega}^2_{(r,s)} = \frac{n^2}{\rho L^2} \frac{\left|\mathbf{K}^*_{(r,s)}\right|}{k^*_{22}k^*_{33} - k^*_{23}k^*_{32}}, \quad r,s = 1,2,\ldots,2n. \tag{26}$$

2.4. Dynamic response

Let a concentrated load of time-dependent magnitude $P(t)$ act at the center of the square plate. Substituting the element loading vectors into Eq. (17) yields

$$\mathbf{f}^*_{(r,s)} = \frac{2P(t)}{n} \sin\frac{r\pi}{2} \sin\frac{s\pi}{2} \begin{Bmatrix} 1 & 0 & 0 \end{Bmatrix}^{\mathrm{T}} = \begin{bmatrix} f^*_1(t) & 0 & 0 \end{bmatrix}^{\mathrm{T}}. \tag{27}$$

Substituting Eq. (25) into Eq. (21) yields

$$\ddot{q}^1_{1(r,s)} + \tilde{\omega}^2_{(r,s)} q^1_{1(r,s)} = f^*_1(t)/\rho a^2, \tag{28a}$$

$$q^2_{1(r,s)} = \frac{f^*_3 k_{23} - f^*_2 k_{33} + (k_{21}k_{31} - k_{23}k_{31}) q^1_{1(r,s)}}{k_{23}k_{32} - k_{22}k_{33}}, \tag{28b}$$

$$q^3_{1(r,s)} = \frac{f^*_3 k_{22} - f^*_2 k_{32} + (k_{21}k_{32} - k_{22}k_{31}) q^1_{1(r,s)}}{k_{22}k_{33} - k_{23}k_{32}}. \tag{28c}$$

Eq. (28a) is a set of second-order differential equation with one variable, and its solution for $q^1_{1(r,s)}$ can be expressed as a Duhamel integral with the initial conditions. $q^2_{1(r,s)}$ and $q^3_{1(r,s)}$ can then be obtained by substituting $q^1_{1(r,s)}$ into Eqs. (28b) and (28c).

Substituting Eq. (27) into Eq. (28a), the solution $q^1_{1(r,s)}$ with zero initial conditions can be expressed as

$$q^1_{1(r,s)} = -\frac{2n}{\tilde{\omega}^2_{(r,s)}\rho L^2} \sin\frac{r\pi}{2} \sin\frac{s\pi}{2} \int_0^t P(\tau) \sin \tilde{\omega}^2_{(r,s)}(t-\tau)\,\mathrm{d}\tau. \tag{29}$$

The response function of the deflection at the center of the plate may be obtained by using Eq. (29) with Eq. (19), i.e.,

$$\tilde{w}_{\mathrm{mid}}(t) = \frac{4}{\rho L^2} \sum_{r=1,3}^{n-1} \sum_{s=1,3}^{n-1} \frac{1}{\tilde{\omega}^2_{(r,s)}} \int_0^t P(\tau) \sin \tilde{\omega}_{(r,s)}(t-\tau)\,\mathrm{d}\tau. \tag{30}$$

The analytical solution obtained by double sine series method may be expressed as

$$w_{\mathrm{mid}}(t) = \frac{4}{\rho L^2} \sum_{r=1,3}^{n-1} \sum_{s=1,3}^{n-1} \frac{1}{\omega^2_{(r,s)}} \int_0^t P(\tau) \sin \omega_{(r,s)}(t-\tau)\,\mathrm{d}\tau, \tag{31}$$

where $\omega_{(r,s)}$ denotes the analytical solution for the natural frequencies. The finite-element solution shown in Eq. (30) converges but does not converge uniformly to the analytical solution (31). The error between Eqs. (30) and (31) is caused because of two main reasons: dividing the continuous plate into equal discrete elements may cause the dispersion errors, and replacing the cyclic mass matrix with the lumped mass matrix neglecting the rotary inertia may cause the interpolation errors.

If the given loading is a simple harmonic force, i.e., $P(t) = Pe^{i\omega' t}$, the integral of the right side of Eq. (30) may be rewritten as

$$\int_0^t Pe^{i\omega'\tau} \sin \tilde{\omega}_{(r,s)}(t-\tau)\,d\tau = \frac{\tilde{\omega}_{(r,s)}\left(e^{i\omega' t} - \cos \tilde{\omega}_{(r,s)}t\right) - i\omega' \sin \tilde{\omega}_{(r,s)}t}{\tilde{\omega}^2_{(r,s)} - \omega'^2}. \tag{32}$$

It is obvious that if the frequency of the load is equal to the natural frequency of the system, a syntonic vibration will occur.

In the following sections, two different types of 12-degree-of-freedom, non-conforming rectangular plate elements are taken as examples to demonstrate the procedure of the presented method.

3. Convergence analysis of the ACM element

Firstly, let us consider the Adini–Clough–Melosh non-conforming plate element (ACM for short) [11]. ACM is a normal 12 DOF rectangular element in plate finite-element analysis, whose shape function is the polynomial space of degree three plus the basic function of two polynomials of degree four. Melosh [12] proved in theory that ACM element can pass the patch test. Long et al. [13] studied its convergence by using the circle conforming condition under a normal stress, and found that ACM element is not only convergent but also in fact a generalized conforming element. This section will discuss its explicit convergence rate and the coefficient of the main error.

Applying the element stiffness matrix $\mathbf{K}^e$ (see Ref. [12]) and the transfer matrix (10) into Eq. (12) yields

$$\mathbf{K}^*_{(r,s)} = \frac{D}{ab}\begin{bmatrix} k_{11} & k_{12} & k_{13} \\ k_{21} & k_{22} & k_{23} \\ k_{31} & k_{32} & k_{33} \end{bmatrix}, \tag{33}$$

where D denotes the flexural rigidity of the plate, and

$$\begin{aligned} k_{11} = {} & \frac{4}{15}\left[60\left(\frac{b}{a}\right)^2 + 60\left(\frac{a}{b}\right)^2 + 42 - 12\mu\right] + \frac{4}{15}\left[-60\left(\frac{b}{a}\right)^2 + 30\left(\frac{a}{b}\right)^2 - 42 + 12\mu\right]\cos r\varphi_1 \\ & + \frac{4}{15}\left[30\left(\frac{b}{a}\right)^2 - 60\left(\frac{a}{b}\right)^2 - 42 + 12\mu\right]\cos s\varphi_2 \\ & + \frac{4}{15}\left[-30\left(\frac{b}{a}\right)^2 - 30\left(\frac{a}{b}\right)^2 + 42 - 12\mu\right]\cos r\varphi_1 \cos s\varphi_2, \end{aligned}$$

$$k_{12} = \bar{k}_{21} = \frac{4}{15}i\left[\left(30\frac{b^2}{a} + 3a - 3a\mu\right)\sin r\varphi_1 + \left(15\frac{b^2}{a} - 3a + 3a\mu\right)\sin r\varphi_1 \cos s\varphi_2\right],$$

$$\begin{aligned} k_{22} = {} & \tfrac{4}{15}(20b^2 + 4a^2 - 4a^2\mu) + \tfrac{4}{15}(10b^2 - a^2 + a^2\mu)\cos r\varphi_1 \\ & + \tfrac{4}{15}(10b^2 - 4a^2 + 4a^2\mu)\cos s\varphi_2 + \tfrac{4}{15}(5b^2 + a^2 - a^2\mu)\cos r\varphi_1 \cos s\varphi_2, \end{aligned}$$

$$k_{32} = \bar{k}_{23} = 0,$$

$$\begin{aligned} k_{33} = {} & \tfrac{4}{15}(20a^2 + 4b^2 - 4b^2\mu) + \tfrac{4}{15}(10a^2 - 4b^2 + 4b^2\mu)\cos r\varphi_1 \\ & + \tfrac{4}{15}(10a^2 - b^2 + b^2\mu)\cos s\varphi_2 + \tfrac{4}{15}(5a^2 + b^2 - b^2\mu)\cos r\varphi_1 \cos s\varphi_2, \end{aligned}$$

$$k_{31} = \bar{k}_{13} = \frac{4}{15}\mathrm{i}\left[\left(-30\frac{a^2}{b} - 3b + 3b\mu\right)\sin s\varphi_2 + \left(-15\frac{a^2}{b} + 3b - 3b\mu\right)\sin s\varphi_2 \cos r\varphi_1\right]. \tag{34}$$

Let a concentrated load P act at the center of the square plate. The maximum deflection can be obtained by substituting Eqs. (14a), (17), (33) and (34) into Eq. (19), i.e.,

$$w_{\mathrm{mid}} = \frac{4PL^2}{D}\left[\frac{A(n)}{\pi^4} + \frac{B(n)}{\pi^2}(n^{-2}) + O(n^{-4})\right] \tag{35}$$

in which

$$A(n) = \sum_{r=1,3}^{n-1}\sum_{s=1,3}^{n-1}\frac{1}{(r^2+s^2)^2}, \quad B(n) = \sum_{r=1,3}^{n-1}\sum_{s=1,3}^{n-1}\frac{r^2s^2(1+\mu)}{6(r^2+s^2)^3}. \tag{36}$$

When n approaches infinity, the coefficient $A(n)$ approaches a constant, i.e., $\lim_{n\to\infty} A(n) = 0.28251$, and the finite solution w_{mid} approaches the exact answer

$$\lim_{n\to\infty} w_{\mathrm{mid}} = \frac{1.1290PL^2}{\mathrm{D}\pi^4}. \tag{37}$$

When n approaches infinity, the finite-element solution for deflection converges to the analytical solution at an asymptotic rate of n^{-2}. The second term on the right-hand side of Eq. (35) presents the main error of the deflection found by the ACM element.

Consider the square plate subjected to a uniformly distributed load with magnitude p_0. For this case, corresponding to Eqs. (14a), (18), (33), (34) and (19), the maximum deflection at the center of the plate may be obtained as

$$w_{\mathrm{mid}} = \frac{16p_0L^4}{D}\left[\frac{A(n)}{\pi^6} + \frac{B(n)}{\pi^4}(n^{-2}) + O(n^{-4})\right] \tag{38}$$

in which

$$A(n) = \sum_{r=1,3}^{n-1}\sum_{s=1,3}^{n-1}(-1)^{(r+s-2)/2}\frac{1}{rs(r^2+s^2)^2}, \quad B(n) = \sum_{r=1,3}^{n-1}\sum_{s=1,3}^{n-1}(-1)^{(r+s-2)/2}\frac{r^4+s^4-2r^2s^2\mu}{12rs(r^2+s^2)^3}. \tag{39}$$

When n approaches infinity, the coefficient $A(n)$ approaches a constant, i.e., $\lim_{n\to\infty} A(n) = 0.244094$, and the finite solution w_{mid} approaches the exact answer

$$\lim_{n\to\infty} w_{\mathrm{mid}} = 3.9055\frac{q_0L^4}{\mathrm{D}\pi^6}. \tag{40}$$

The first term on the right-hand side of Eq. (38) represents the limiting solution which is in agreement with the analytical solution. Then the second term represents the main error of the deflection found by the ACM element. When n approaches infinity, the deflection converges to the analytical solution at an asymptotic rate of n^{-2}. Some numerical results for Eq. (35) and (38) are given in Table 1. It can be known from Table 1 that when n increases, the deflections approach the analytical solutions and the relative errors decrease fast.

Substituting Eqs. (33) and (34) into Eq. (26), and expanding the right side into a power series of ψ, we gain the natural frequencies

$$\tilde{\omega}^2_{(r,s)} = \frac{D\pi^4}{\rho L^4}\left[A(n) + \pi^2 B(n)(n^{-2}) + O(n^{-4})\right] \tag{41}$$

in which

$$A(n) = (r^2+s^2)^2, \quad B(n) = -\frac{r^2s^2(r^2+s^2)(1+\mu)}{6}. \tag{42}$$

Eq. (41) shows that the natural frequencies found by the ACM element converge to the exact solutions at an asymptotic rate of n^{-2} when n approaches infinity. Some numerical results for Eq. (41) are given in Table 2.

Table 1
Central deflections w_{mid} by ACM element ($\mu = 0.3$)

n	2	4	8	16	32	∞
Under concentrated load	0.01301 (0.06683)[a]	0.01208 (0.02097)	0.01176 (0.00635)	0.01165 (0.00187)	0.01162 (0.00054)	0.011601
Under uniform load	0.00356 (−0.03598)	0.00395 (−0.00648)	0.00403 (−0.00172)	0.00406 (−0.00043)	0.00406 (−0.00011)	0.004062
Multiplier	Concentrated load: PL^2/D, uniform load: p_0L^4/D					

[a]Numbers in the parentheses denote the relative errors.

Table 2
Natural frequencies $\tilde{\omega}^2_{(r,s)}$ by ACM element ($\mu = 0.3$)

n	2	4	8	16	32	∞
(1,1)	285.4859 (−0.26730)[a]	363.5987 (−0.06683)	383.1270 (−0.01671)	388.0090 (−0.00418)	389.2295 (−0.00104)	389.6364
(1,2), (2,1)		2174.851 (−0.10692)	2370.133 (−0.02673)	2418.954 (−0.00668)	2431.159 (−0.00167)	2435.227
(2,2)		4567.739 (−0.26730)	5817.580 (−0.06683)	6130.031 (−0.01671)	6208.144 (−0.00418)	6234.182
Multiplier	$D/\rho L^4$					

[a]Numbers in the parentheses denote the relative errors.

4. Convergence analysis of the M element

Consider now the convergence of four nodes and 12-degree-of-freedom Mindlin non-conforming plate element (M for short) [14]. The displacements and rotations of the element have their own shape functions and are interpolated independently. It contains the shear deformation, and its expression is similar to that of plane stress element. The M element is of simple formulation and high precision, and can be used to analyze both thin plate and heavy plate, so it is applied widely in structural analysis. But the study on the convergence of the M element is few. This section will discuss the convergence rate and the coefficient of the main error of four nodes rectangular M element.

Substituting the stiffness matrix $\mathbf{K}^e$ (see Ref. [14]) and the transfer matrix (10) into Eq. (12) yields

$$\mathbf{K}^*_{(r,s)} = \frac{D}{ab}\begin{bmatrix} k_{11} & k_{12} & k_{13} \\ k_{21} & k_{22} & k_{23} \\ k_{31} & k_{32} & k_{33} \end{bmatrix} \tag{43}$$

in which

$$k_{11} = 4\left[6\left(\frac{b}{a}\right)^2 + 6\left(\frac{a}{b}\right)^2 + \frac{72}{16}\mu + 2 - 2\mu\right] + 4\left[-6\left(\frac{b}{a}\right)^2 - \frac{72}{16}\mu - 2 + 2\mu\right]\cos r\varphi_1 + 4\left[-6\left(\frac{a}{b}\right)^2 - \frac{72}{16}\mu - 2 + 2\mu\right]\cos s\varphi_2 + 4\left[\frac{72}{16}\mu + 2 - 2\mu\right]\cos r\varphi_1 \cos s\varphi_2,$$

$$k_{12} = \bar{k}_{21} = 4\mathrm{i}\left[\left(3\frac{b^2}{a} + \frac{6}{16}a\mu\right)\sin r\varphi_1 - \frac{6}{16}a\mu \sin r\varphi_1 \cos s\varphi_2\right],$$

$$k_{22} = 4\left[2b^2 + b^2 \cos r\varphi_1\right],$$

$$k_{32} = \bar{k}_{23} = \frac{ab}{4}\mu \sin r\varphi_1 \sin s\varphi_2,$$

$$k_{33} = 4\left[2a^2 + a^2 \cos s\varphi_2\right],$$

$$k_{31} = \bar{k}_{13} = \frac{4}{15}\mathrm{i}\left[\left(-30\frac{a^2}{b} - 3b + 3b\mu\right)\sin s\varphi_2 + \left(-15\frac{a^2}{b} + 3b - 3b\mu\right)\sin s\varphi_2 \cos r\varphi_1\right]. \tag{44}$$

In a manner similar to Section 3, we can study the convergence of the finite-element solution of the M element. Consider now the plate subjected to a concentrated load of magnitude P. Substituting Eqs. (14a), (17), (43) and (44) into Eq. (19) yields

$$w_{\mathrm{mid}} = \frac{4PL^2}{D}\left[\frac{A(n)}{\pi^4} + \frac{B(n)}{\pi^2}(n^{-2}) + O(n^{-4})\right] \tag{45}$$

in which

$$A(n) = \sum_{r=1,3}^{n-1}\sum_{s=1,3}^{n-1}\frac{1}{(r^2+s^2)^2}, \quad B(n) = \sum_{r=1,3}^{n-1}\sum_{s=1,3}^{n-1}\frac{r^2s^2(\mu^2-4\mu+8)}{48(r^2+s^2)^3}. \tag{46}$$

It is obvious that when n approaches infinity, the solution (45) converges to the exact deflection (37) at an asymptotic rate of n^{-2}. Comparing Eq. (35) with Eq. (45), it can be found that under a same concentrated load, the solutions found by the ACM element and the M element converge to the same exact answer at a same asymptotic rate, but the coefficients of main errors are different. It may be verified that $\lim_{n\to\infty}(B(n)_{\mathrm{ACM}}/B(n)_{\mathrm{M}}) = 1.5094$, i.e., the solution by the M element converges faster than that by the ACM element.

Consider the case of the plate subjected to a uniformly distributed load with magnitude p_0. Substituting Eqs. (14a), (18), (43) and (44) into Eq. (19), yields

$$w_{\mathrm{mid}} = \frac{16p_0L^4}{D}\left[\frac{A(n)}{\pi^6} + \frac{B(n)}{\pi^4}(n^{-2}) + O(n^{-4})\right] \tag{47}$$

in which

$$A(n) = \sum_{r=1,3}^{n-1}\sum_{s=1,3}^{n-1}(-1)^{(r+s)/2}\frac{1}{rs(r^2+s^2)^2},$$

$$B(n) = \sum_{r=1,3}^{n-1}\sum_{s=1,3}^{n-1}(-1)^{(r+s-2)/2}\frac{4r^4+4s^4-r^2s^2(\mu^2-4\mu)}{48rs(r^2+s^2)^3}. \tag{48}$$

It may be found that when n approaches infinity, the maximum deflection (47) converges to the analytical solution (40) at an asymptotic rate of n^{-2}. The second term on the right-hand side of Eq. (47) presents the main error of the deflection found by the M element. Some numerical results for Eqs. (45) and (47) are given in Table 3.

From Tables 1 and 3, it is obvious that under a same uniformly distributed load the maximum deflections found by the ACM element and the M element converge to the same exact solution at a same asymptotic rate. When $\mu = 0.3$, the relative error of the M element solution is smaller than that of the ACM element solution, so the former converges faster.

Table 3
Central deflections w_{mid} by M element ($\mu = 0.3$)

n	2	4	8	16	32	∞
Under concentrated load	0.01208 (0.04427)[a]	0.01178 (0.01389)	0.01167 (0.00421)	0.01163 (0.00124)	0.01161 (0.00036)	0.011601
Under uniform load	0.00383 (−0.01998)	0.00389 (−0.00427)	0.00404 (−0.00109)	0.00406 (−0.00027)	0.00406 (−0.00007)	0.004062
Multiplier	Concentrated load: PL^2/D, uniform load: p_0L^4/D					

[a]Numbers in the parentheses denote the relative errors.

Table 4
Natural frequencies $\tilde{\omega}^2_{(r,s)}$ by M element ($\mu = 0.3$)

n	2	4	8	16	32	∞
(1,1)	320.6367 (−0.17709)[a]	372.3864 (−0.04427)	385.3239 (−0.01107)	388.5582 (−0.00277)	389.3668 (−0.00069)	389.6364
(1,2), (2,1)		2262.728 (−0.07083)	2392.102 (−0.01771)	2424.446 (−0.00443)	2432.532 (−0.00111)	2435.227
(2,2)		5130.187 (−0.17709)	5958.183 (−0.04427)	6165.182 (−0.01107)	6216.932 (−0.00277)	6234.182
Multiplier	$D/\rho L^4$					

[a]Numbers in the parentheses denote the relative errors.

Comparing the maximum deflection under uniform load by the ACM element, which is expressed in Eq. (38), with the exact deflection found by the finite-difference method (see Ref. [6]), it may be found that the two solutions converge at a same asymptotic rate, i.e., n^{-2}. But the main error of the ACM element solution is smaller, so it converges faster. In other words, the solutions by the ACM element and the M element converge faster than the finite-difference solutions.

The expression of the natural frequencies by the M element may be obtained by substituting Eqs. (43) and (44) into Eq. (26), i.e.,

$$\tilde{\omega}^2_{(r,s)} = \frac{D\pi^4}{\rho L^4}\left[\frac{A(n)}{\pi^4} + \frac{B(n)}{\pi^2}(n^{-2}) + O(n^{-4})\right] \tag{49}$$

in which

$$A(n) = (r^2 + s^2)^2, \quad B(n) = -\frac{r^2s^2(r^2 + s^2)(\mu^2 - 4\mu + 8)}{48}. \tag{50}$$

The natural frequencies found by the M element converge from below the exact answers at an asymptotic rate of n^{-2} when n approaches infinity. Some numerical results for Eq. (49) are given in Table 4.

Comparing Eq. (41) with Eq. (49), it may be found that the natural frequencies found by the ACM element and M element converge to the same exact answer at a same asymptotic rate, but the coefficients of the main errors are different. It may be verified that the solution by the M element converges faster than that by the ACM element. This conclusion may also be derived from Tables 2 and 4.

5. Conclusions

The present paper investigated the convergence problems of two non-conforming plate elements in structural analysis. After using the double U-transformation, the finite-element equations are uncoupled to

a set of independent equations, and then the analytical finite-element solutions for the maximum deflections under different loading function and natural frequencies are obtained easily. The results show that the solutions of ACM and M element converge to the exact answer at a same asymptotic rate, but the coefficients of main errors are different. Comparing the main errors, it can be found that the M element converges faster than the ACM element. The method presented in this paper may be applied to study the exact solutions of rectangular plates with other supported edges. In the cases, the equivalent systems must be established in other ways.

Acknowledgments

This work is supported in part by the TRAPOYT, NSFC, CPSF and the Foundation of Zhongshan University Advanced Research Centre.

References

[1] Y.K. Cheung, H.C. Chan, C.W. Cai, Exact method for static analysis of periodic structures, *Journal of Engineering Mechanics* 115 (1989) 415–434.
[2] C.W. Cai, Y.K. Cheung, H.C. Chan, Uncoupling of dynamic equations for periodic structures, *Journal of Sound and Vibration* 139 (1990) 253–263.
[3] L. Gao, J.K. Liu, Uncoupling of governing equations for cyclic bi-periodic structures, *Advances in Structures Engineering* 4 (2001) 137–145.
[4] C.W. Cai, J.K. Liu, Y. Yang, Exact analysis of localized modes in two-dimensional bi-periodic mass-spring systems with a single disorder, *Journal of Sound and Vibration* 288 (2005) 307–320.
[5] J.K. Liu, Y. Yang, M. Cai, Convergence study of the finite difference method: a new approach, *Acta Mechanica Sinica* 35 (2003) 757–760.
[6] J.K. Liu, Y. Yang, C.W. Cai, Convergence studies on static and dynamic analyses of plates by using the U-transformation and the finite difference method, *Journal of Sound and Vibration* 289 (2006) 66–76.
[7] H.C. Chan, C.W. Cai, Y.K. Cheung, Convergence studies of dynamic analysis by using the finite element method with lumped mass matrix, *Journal of Sound and Vibration* 165 (1993) 193–207.
[8] O.C. Zienkiewicz, R.L. Taylor, *The Finite Element Method*, fourth ed., McGraw-Hill, London, 1991.
[9] C.W. Cai, J.K. Liu, Y. Yang, Exact analysis of localized modes in two-dimensional bi-periodic mass-spring systems with a single disorder, *Journal of Sound and Vibration* 288 (2005) 307–320.
[10] C.W. Cai, J.K. Liu, H.C. Chan, *Exact Analysis of Bi-Periodic Structures*, World Scientific, Singapore, 2002.
[11] P. Lascaux, P. Lesaint, Some nonconforming finite elements for plate bending problems, *RAIRO Numerical Analysis* 9 (1975) 9–53.
[12] R.J. Melosh, Basis for derivation of matrices for the direct stiffness method, *AIAA Journal* 1 (1963) 1631–1637.
[13] Y.Q. Long, Z.F. Long, S. Cen, *Theory on New Type Finite Elements*, Tsinghua University Press, Beijing, 2004.
[14] E. Hintone, H.C. Huang, A family of quadrilateral Mindlin plate elements with substitute shear strain fields, *Computers & Structures* 23 (1986) 409–431.